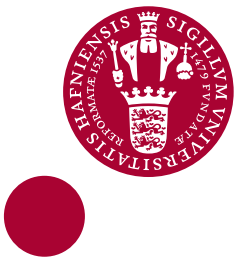

Sedimentology, carbon isotope stratigraphy and micropalaeontology of the Rhaetian Zlambach Formation-Implications for the Dachstein carbonate platform development (Northern Calcareous Alps, Austria)

Mette, Wolfgang; Clemence, Marie-Emilie; Thibault, Nicolas; Korte, Christoph; Konrad, Bernadette; Ullmann, Clemens Vinzenz

Published in:
Sedimentary Geology

DOI:
10.1016/j.sedgeo.2018.12.009

Publication date:
2019

Document version
Publisher's PDF, also known as Version of record

Sedimentary Geology 382 (2019) 47–60

Contents lists available at ScienceDirect

Sedimentary Geology

journal homepage: www.elsevier.com/locate/sedgeo

Sedimentology, carbon isotope stratigraphy and micropalaeontology of the Rhaetian Zlambach Formation– Implications for the Dachstein carbonate platform development (Northern Calcareous Alps, Austria)

Wolfgang Mette [a,*], Marie-Emilie Clemence [a], Nicolas Thibault [b], Christoph Korte [b], Bernadette Konrad [a], Clemens Vinzenz Ullmann [c]

[a] Institut für Geologie, University of Innsbruck, Innrain 52, 6020 Innsbruck, Austria
[b] Department of Geosciences and Natural Resource Management, University of Copenhagen, Øster Voldgade 10, 1350 Copenhagen, Denmark
[c] University of Exeter, Camborne School of Mines, College of Engineering, Mathematics and Physical Sciences, Penryn, Cornwall TR10 9FE, UK

ARTICLE INFO

Article history:
Received 21 August 2018
Received in revised form 20 December 2018
Accepted 21 December 2018
Available online 18 January 2019

Editor: Dr. B. Jones

Keywords:
Rhaetian
Northern Calcareous Alps
Carbon isotopes
Sequence stratigraphy
Microfossils

ABSTRACT

Middle to late Rhaetian toe–of–slope to basin deposits (Zlambach Formation) of the Northern Calcareous Alps in the Tethyan realm have been studied with respect to depositional palaeoenvironments and chemo- and sequence stratigraphy, using high-resolution stable isotope and X-ray fluorescence measurements, microfacies and microfossil analysis. Our results show that the Zlambach Formation represents a regressive-transgressive succession which includes one 3rd order and two 4th order depositional sequences as well as several subordinate sedimentary cycles reflecting variations of calciturbidite input from the Dachstein platform due to minor sea-level fluctuations. We present the first high-resolution $\delta^{13}C_{carb}$ record for the Middle and Upper Rhaetian interval of the west Tethyan open marine realm. The data show, in contrast to earlier suggestions, that growth and progradation of the Dachstein carbonate platform margin was continuous until the early *Choristoceras marshi* ammonoid zone (upper Rhaetian). In the late *C. marshi* zone the Hallstatt basin was affected by significant environmental perturbations as recorded by a 1.0‰ C_{carb} negative excursion followed by a 1.3‰ positive excursion and contemporaneous fluctuations in benthic microfossil abundance and diversity. The occurrence of comparable carbon isotope excursions in the late *C. marshi* zone of intraplatform basinal deposits of the Northern Calcareous Alps suggests that these perturbations were of a higher significance than previously thought. These isotope excursions could be related to regional ecologic changes such as the late Rhaetian termination of the Dachstein platform margin growth.

1. Introduction

The Late Triassic has been intensively studied in recent years with respect to carbon isotope stratigraphy. Most of these studies (e.g. Hesselbo et al., 2002; Kürschner et al., 2007; Pálfy et al., 2007; Ruhl et al., 2009; Korte and Kozur, 2011; Pálfy and Zajzon, 2012; Felber et al., 2015; see also Korte et al., 2019 for an overview) focussed on the Triassic/Jurassic boundary interval where one of the largest global extinction events of the Phanerozoic is documented and which is characterised by distinct global negative carbon isotope excursions. However, the carbon isotope stratigraphy of the Rhaetian (e.g. Korte et al., 2005; Richoz et al., 2012; Whiteside and Ward, 2011; Mette et al., 2012; Korte et al., 2017; Zaffani et al., 2018) in general and the late Rhaetian pre-extinction interval in particular still lacks sufficient resolution. This is largely due to the fact that there are few continuous Rhaetian sections in open marine settings were the bulk carbonate carbon isotope ($\delta^{13}C_{carb}$) record was not affected by diagenesis or other factors. The only complete Rhaetian $\delta^{13}C_{carb}$ curves from western Tethyan pelagic environments published so far were reported from Italian sections. Muttoni et al. (2014) published a $\delta^{13}C_{carb}$ curve of moderate resolution from the southern Alps, showing very large negative and positive excursions which were interpreted as probably caused by mixing of shallow marine carbonate sediments from different sources. Rigo et al. (2015) showed $\delta^{13}C_{carb}$ and $\delta^{13}C_{org}$ records of much lower stratigraphic resolution from pelagic deposits of the southern Appennines reaching up to the middle or late Rhaetian (*Misikella ultima* conodont zone). In the Northern Calcareous Alps, the Rhaetian is represented in continuous successions of intraplatform basinal environments (Kössen Formation) and in oceanic basin successions of the western Tethys (Zlambach Formation). A $\delta^{13}C_{carb}$ record of low to moderate resolution from the lower to middle Rhaetian part of the Zlambach Formation was reported by Richoz et al. (2012). Subsequent carbon isotopic studies (Mette et al., 2012; Korte et al., 2017) of Rhaetian intraplatform basin

* Corresponding author.
E-mail address: Wolfgang.Mette@uibk.ac.at (W. Mette).

https://doi.org/10.1016/j.sedgeo.2018.12.009

facies have shown that significant carbon isotope excursions occurred in the late Rhaetian. It is, however, not clear whether these isotope excursions were just the result of regional environmental changes or if they reflect a more significant perturbation of the global carbon cycle (see discussion in Korte et al., 2017). The intention of the present study is therefore to document the carbon isotope record at high resolution as well as the sedimentary succession and palaeoenvironmental changes in the Rhaetian open marine realm of the western Tethys.

2. Geological setting

During the late Paleozoic to early Mesozoic, the Hallstatt facies (Northern Calcareous Alps, NCA) was located at the western termination of the Neotethys (Mandl, 2000; Haas et al., 2010; Fig. 1a). In the Late Triassic (Rhaetian), the distal shelf deposits of the western Tethyan margin included the Dachstein platform system in the northwest and the Hallstatt deeper shelf and basin in the southeast (Fig. 1a, b).

The opening of the Neotethys Ocean led to the development of extensional basins and carbonate platforms in the Middle Triassic (Mandl, 2000). A transgressive pulse just before the Carnian/Norian boundary caused an onlap of pelagic limestones over the shallow water carbonates and initiated the rapid growth of the thick Norian carbonate platform (Mandl, 2000; Fig. 1b). In the Hallstatt facies zone (Fig. 1c), the pelagic onlap represents a short time interval and open marine deposits became covered by the prograding carbonate platform of the Dachstein Limestone (Fig. 1b).

In the Rhaetian the Dachstein platform is bordered in the Northwest by an extensive shallow shelf with patch reef deposits (Oberrhaet Limestone) and an intraplatform basin where the Kössen Formation was deposited. The reefs of the southeastern Dachstein platform margin are interfingering with resedimented Norian limestones (Pedata Limestone) and the Rhaetian Zlambach Formation (Fig. 1b, c). The Late Carnian-Norian Pötschen Limestone and the Zlambach Formation represent the basinal part of the open marine deeper Hallstatt shelf in the Neotethys (Mandl, 2000; Richoz et al., 2012). The Zlambach Formation includes a lower 30–40 m thick unit of alternating grey marls ("Untere Zlambach-Schichten"), bioturbated and fossiliferous micricitic limestones, allochthonous arenitic limestones and an upper monotonous unit of dark shales and marls with pyrite nodules and 0,5–1 m thick bioturbated marly limestones ("Obere Zlambach-Schichten") (Krystyn, 1987, 1991; Matzner, 1986). The thickness of the upper unit cannot be determined due to pervasive tectonism. Estimates vary between a minimum of 25 m and a maximum of 100 m.

The studied sections of the Rhaetian Zlambach Formation are located in the NCA, about 4 km east of Bad Goisern (Salzkammergut, Austria), near Rossmoosalm (Fig. 1d). Two sections were investigated with approximately 500 m distance along a WNW–ESE transect, section 1 [47°39′10.79″ N 13°38′48.59″ E] and section 2 [47°39′01.01″ N 13°39′10.61″ E] (Fig. 1d).

The bio- and lithostratigraphy of section 1 (~41 m thick; Fig. 2) were studied by Piller (1978), Krystyn (1987) and Weiland (1991). Based on their data and our additional ammonite occurrences, section 1 is attributed to the middle Rhaetian (*Vandaites stuerzenbaumi* ammonoid Zone) and lower upper Rhaetian (lower *C. marshi* ammonoid Zone; see Figs. 2, 3). Section 2 (~23 m thick; Fig. 3) is dated as upper Rhaetian (upper *C. marshi* zone) on the basis of the occurrence of *C. marshi*. The lithology shows a distinct overlapping interval of ~8 m thickness between the uppermost part of section 1 and the lower part of section 2 (Fig. 3). In section 1, the litho- and biostratigraphy data thereby allow to calibrate the high-resolution $\delta^{13}C_{carb}$ curve reported later in this study (Fig. 3).

In the lowermost part of the Rossmoosgraben composite section (0–11 m interval), attributed to the *V. stuerzenbaumi* zone, compact clayey limestone beds (10–20 cm) are intercalated with thin light-

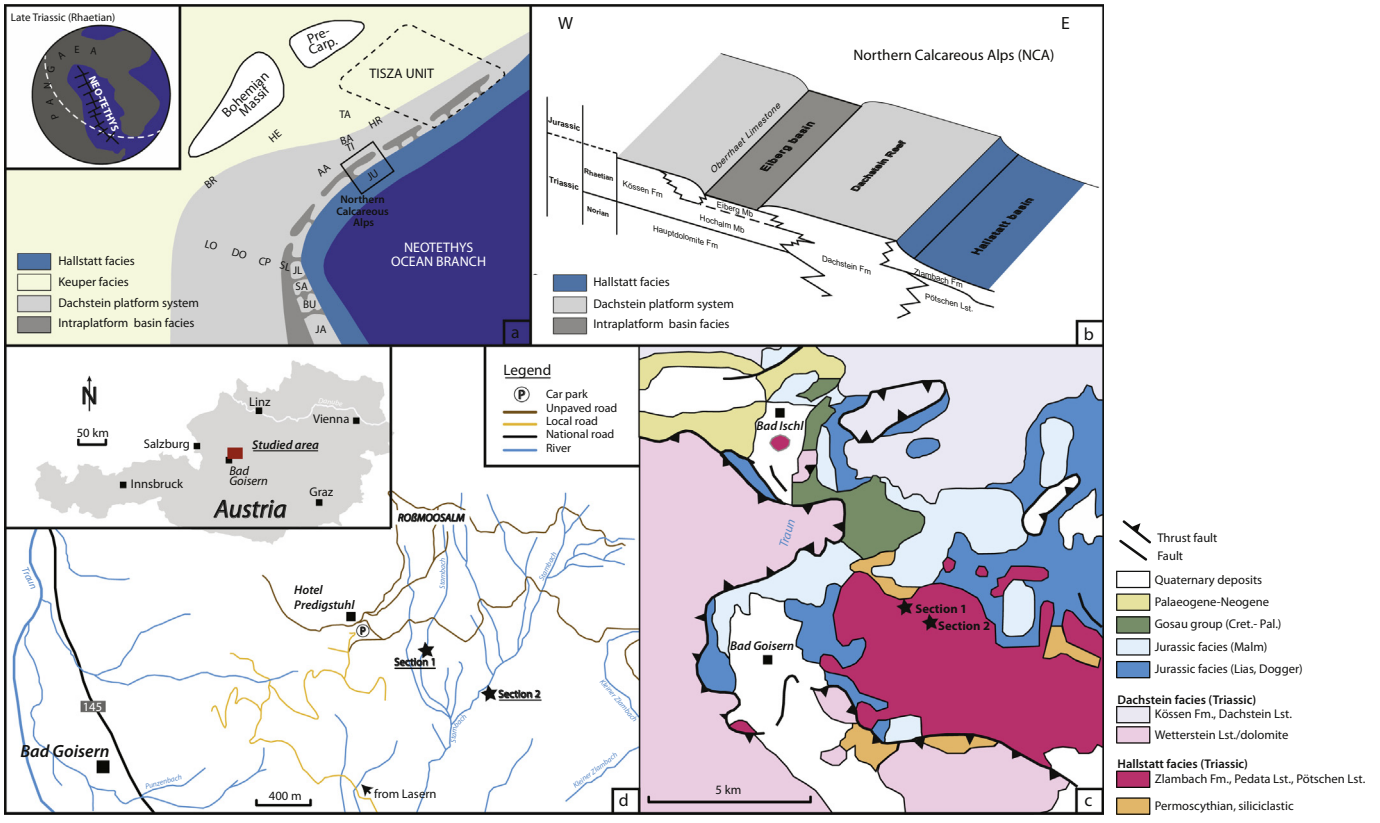

Fig. 1. (a) Palaeogeographic reconstruction for the Western Tethyan margin during the Late Triassic (modified after Hornung et al., 2008). (b) Map showing the location of the Rossmoosgraben sections and geological setting in Northern Calcareous Alps (modified after Kürschner et al., 2007). (c) Geological map (simplified after Schäfer, 1982). (d) Locality map of the studied sections.

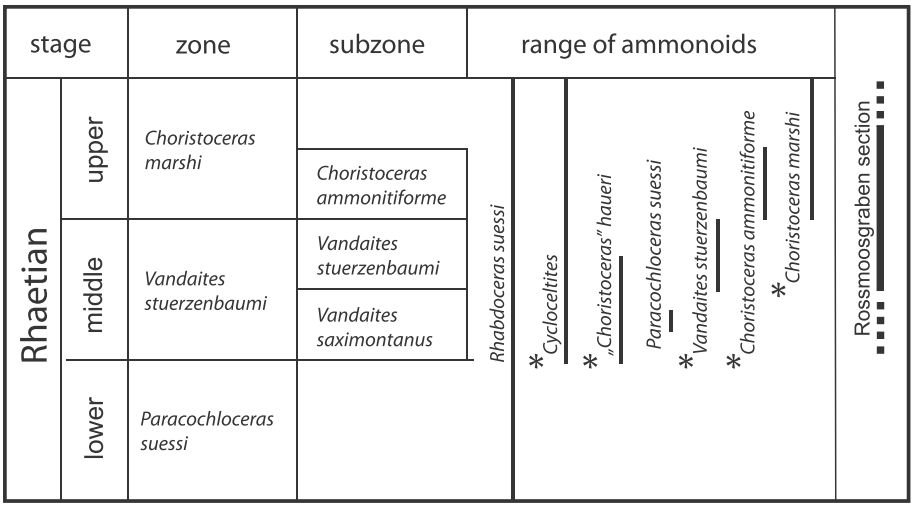

Fig. 2. Rhaetian ammonoid zonation of the Tethyan realm (according to Krystyn, 1987, 1990; Maslo, 2008) and stratigraphic range of the Rossmoosgraben section (*ammonoids occurring at Rossmoosgraben section).

grey bioturbated marl layers and dark shale beds (20–50 cm) (Figs. 3, 4) representing the lower unit of the Zlambach Formation. The bioturbated layers contain abundant and low diversified trace fossils (*Chondrites* sp., *Planolites* sp., *Zoophycos* sp., and *Thalassinoides* sp.) as well as few macrofauna, including ammonites and shell fragments of pelagic bivalves and brachiopods. The *C. ammonitiforme* subzone of the *C. marshi* zone (11–29 m interval) shows stacked thickening-upward sequences (2–4 m) of thicker bioturbated limestone beds (30–40 cm) and light-grey bioturbated marl and dark shale (>1 m) couplets. In the upper third of the section (*C. marshi* subzone, 29–56 m interval), the Zlambach Formation shows few marly limestone beds and a transition of light-grey marl layers to dark marly shales representing the upper unit of the Zlambach Formation. The light-grey clayey marls are partly laminated in the lower part and become increasingly bioturbated and dark towards the upper part of the *C. marshi* zone, above 45 m (Fig. 4).

3. Material and methods

3.1. Microfacies analysis

Eighty one samples were taken to characterise the microfacies using the classification scheme of Dunham (1962) and the rock constituents. For a more detailed description of the very fine-grained carbonate types the terminologies of Folk (1959) and Grabau (1904) have been applied. The sampling intervals are indicated in Fig. 4. Based on field observations and detailed microfacies investigations, different lithofacies types have been distinguished.

3.2. Analytical procedure

A total of 652 samples were collected for stable isotope analysis and XRF measurements: 339 samples from section 1 and 313 samples from section 2 at vertical sample spacing of ~5–10 cm. The resulting composite curve consists of 582 data points in total.

3.2.1. Stable isotope analysis

The bulk rock samples for $\delta^{13}C_{carb}$ and $\delta^{18}O_{carb}$ analyses were performed on a ThermoFisher Delta^{Plus}XL isotope ratio mass spectrometer with an analytic precision (1σ) of 0.08‰ for $\delta^{18}O_{carb}$ and 0.06‰ for $\delta^{13}C_{carb}$ (Spötl and Vennemann, 2003; Institute of Geology, University of Innsbruck), reported on the V-PDB scale and calibrated against NBS19.

3.2.2. Hand-held XRF measurements

Geochemical composition of the bulk rock powders was measured using a handheld energy dispersive X-Ray Fluorescence (XRF) spectrometer alpha-8000 LZX from Innov–X/Olympus (Dahl et al., 2013) in the department of Geosciences and Natural Resource Management (IGN), University of Copenhagen. Powders were measured directly in their cylindrical containers (Diameter = 3 cm; Height = 6.5 cm; ≥2.5 cm thick layer of powder) by covering the opening with a thin layer of kitchen wrap. Conversion from absorption to concentrations was performed after calibration at stainless steel target and subsequent data reduction was obtained using Innov–X software that included a five-point calibration curve with NIST standards (NIST 2702, NIST 2709, NIST 2710, NIST 2711, NIST 2781). Internal lab calibration of the device is described in Ahm et al. (2017) and the fully detailed recommended procedure for analysis is given in Thibault et al. (2018). Comparison of XRF versus ICP-MS measurements shows that the average relative external uncertainty across all recorded elements is within 13%, and the intrumental error is generally less than 10% (Ahm et al., 2017). A wide range of elements heavier than Na is automatically detected and quantified during XRF analysis.

3.3. Microfossil analysis

For micropalaeontological analysis 37 samples of shales and marls have been dissolved using a standard laboratory method. Each sample was dried at 80 °C and 500 g of sediment was treated with petroleum and 15% hydrogen peroxide. The dissolved residue was washed with sieves of 1.0 mm, 0.3 mm, 0.1 mm and 0.063 mm mesh-size. The residue of prepared samples was completely picked and used for a quantitative ostracod analysis. For the abundance analysis two complete valves or one complete carapace were counted as one specimen. For the population age structure analysis the total number of specimens of each juvenile stage and the adult stage of the species *Ogmoconcha amphicrassa* (Kristan-Tollmann, 1971) was determined. The taphonomic interpretation of the age structure was based on Whatley (1988) and Boomer et al. (2003). The ecological diversity was evaluated using the Shannon-Wiener diversity index.

4. Sedimentological and geochemical results

4.1. Microfacies analysis

Based on the microfacies analysis of the Rhaetian Zlambach Formation of Rossmoosgraben, four lithofacies types (LF1, LF2, LF3 and LF4)

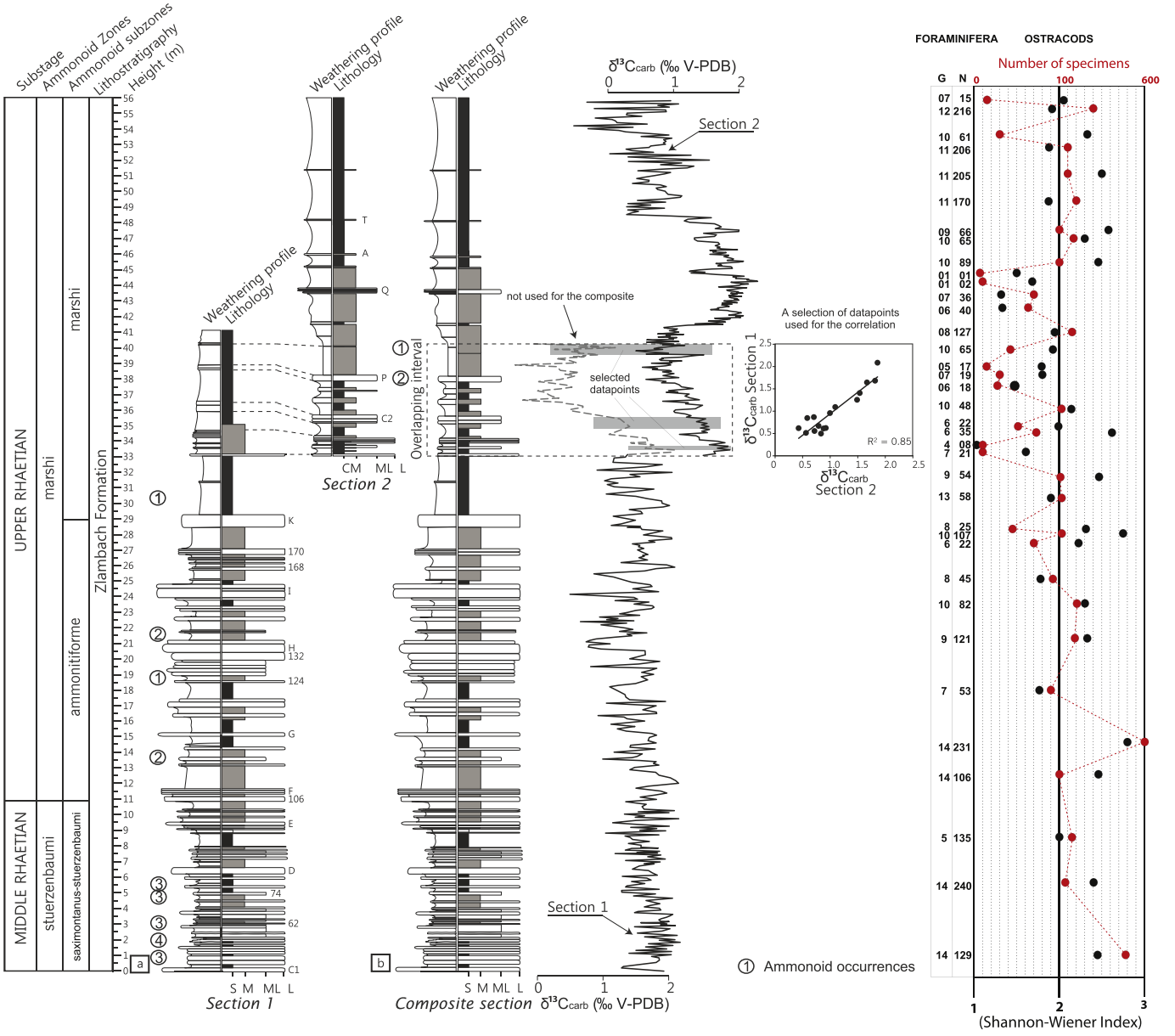

Fig. 3. Biostratigraphy, lithostratigraphy and carbon isotope record of the Zlambach Formation at the Rossmoosgraben sections (S = shales, M = marls, ML = marly limestones, L = limestones); ostracod total abundance (number of specimens) and species diversity (Shannon—Wiener Index); foraminifera total abundance (N = number of specimens) and diversity (G = number of genera). The uppermost part of section 1 and the lower part of section 2 show a litho- and isotope stratigraphic congruence. A composite section of the Zlambach Formation at Rossmoosgraben has been constructed based on a significant correlation between the $\delta^{13}C_{carb}$ curve of sections 1 and 2 ($R^2 = 0.85$). Ammonoid occurrences (this study): 1 = *Choristoceras* cf. *marshi*, 2 = *Choristoceras* sp., 3 = *Cycloceltites arduini*, 4 = *Gigantarcestes*? sp. (det. L. Krystyn). The range of the *V. stuerzenbaumi* zone and the *C. ammonitiforme* subzone is based on data of Weiland (1991).

were defined. The most important characteristics of the distinguished facies types, together with their interpreted depositional setting, are illustrated in Fig. 4 and summarized in Table 1. For each LF type the corresponding standard microfacies types of Flügel (2004) is quoted.

4.1.1. LF1 – Medium-grained peloid-bioclast grainstone (Fig. 4/A–D)

The microsparitic matrix contains densely packed peloids (Fig. 4/A). In general maximum diameters of bio- and lithoclasts reach 150 μm. Echinoderm fragments might exceed the size limits because of their special hydrodynamic behaviour. Among the bioclasts, agglutinated foraminifers, ostracods and radiolarians dominate (Fig. 4/B–C). Rare fragments of echinoderms and calcareous foraminifers are also observed (Fig. 4/D). The presence of silt-size terrigenous siliciclastics (i.e., quartz) also characterizes this lithofacies type. It corresponds to Standard Microfacies type (SMF) 2 of Flügel (2004).

4.1.2. LF2 – Medium-grained peloid-bioclast packstone to wackestone (Fig. 4/E–L)

It consists of laminated strata made up of graded, fine calcarenite packstones (60–150 μm) and wackestone (40–70 μm) (Fig. 4/E–H). The calcarenite laminae are peloidal and contain diverse bioclasts (fragments of echinoderms, ostracods, agglutinated foraminifers, and radiolarians (Fig. 4/F, I–L). The thin lamination is marked by levels where the micritic matrix is recrystallized into microsparite. The wackestone shows faintly parallel silty laminations, commonly grading upwards into mudstone (Fig. 4/G–H). The wackestone is dominantly composed of radiolarians (usually calcite moulds) associated with rare

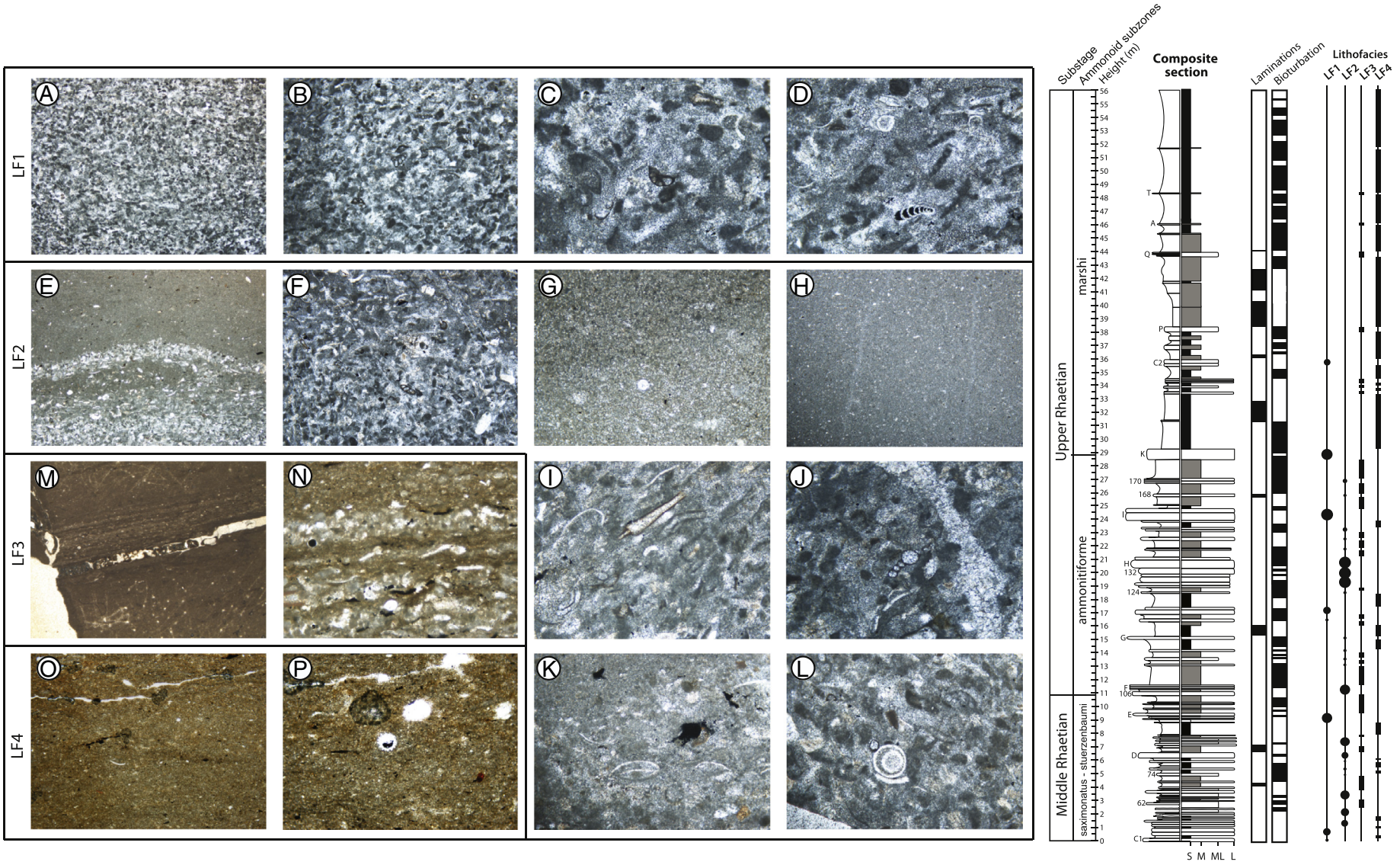

Fig. 4. Lithostratigraphy, sedimentary structures (lamination, bioturbation) and carbonate microfacies types (LF 1-4) of the Zlambach Formation at the Rossmoosgraben composite section. (LF 1: A-D, LF 2: E-L, LF 3: M-N, LF 4: O-P); (S = shales, M = marls, ML = marly limestones, L = limestones).

Table 1
Carbonate lithofacies types of the Zlambach Formation at Rossmoosgraben section and their depositional environment.

Lithofacies	Constituents and their palaeoenvironment		Interpretations		Depositional setting
Lf1[1]- Medium-grained peloid-bioclast grainstone	Benthic agglutinated foraminifera[1,2] Peloids[1,2,3,4]	**Platform interior**	**Distal turbidites**	Suspension deposition from a low-density turbidity current	**Distal toe-of-slope**
Lf2[2]- Medium-grained peloid-bioclast packstone - wackestone	Benthic agglutinated foraminifera[1,2] (*Glomospira* sp., *Glomospirella* sp., *Ophtalmidium* sp., *Planiinvoluta* sp., *Agathammina* sp., *Earlandia* sp., *Duotaxis* sp., *Meandrospira* sp., *Rectocornuspira* sp.)	**Shallow reef**		Suspension deposition from a low density turbidity current	
Lf3[3]- Peloid wackestone to mudstone	Thin-shelled benthic hyaline foraminifera (Nodosariids, *Lenticulina* sp.)[1,2] Thin-shelled ostracods[1,2,3,4] Radiolarians[1,2,3,4] Sponge spicules[2,3,4]	**Open ocean**		Suspension deposition from a very distal low density current	**Basin**
Lf4[4]- Mudstone	LF1[1],LF2[2],LF3[3],LF4[4]			Radiolarian facies Fall-out of „background" pelagic suspension	

fragments of echinoderms and sponge spicules (Fig. 4/G) and is transitional between SMF 1 and 2 (Flügel, 2004).

4.1.3. LF3 – Peloid wackestone to mudstone (Fig. 4/M–N)

Fine peloidal calcarenite–calcisiltite laminae alternate with peloidal microsparite and micrite (Fig. 4/M). It is poor in recognisable bioclasts (mainly radiolarians and rare thin-shelled ostracods and sponge spicules; Fig. 4/N). The peloids are tiny (~50 μm) globular micritic particles (Fig. 4/N). LF3 is transitional between SMF 1 and 2 (Flügel, 2004).

4.1.4. LF4 – Mudstone (Fig. 4/O–P)

This microfacies type is homogeneous in structure and composition. Homogeneous micritic matrix predominates (Fig. 4/O). In some cases, lamination is recognisable. Peloids and fine bioclasts are very rare (radiolarians, sponge spicules and thin-shelled ostracods; Fig. 4/P). LF4 corresponds to SMF 1 (Flügel, 2004).

4.2. Elemental geochemical analysis

In order to characterise changes in the chemical composition of the lithofacies described above which are not caused by dilution of $CaCO_3$, trace elements were plotted as ratios normalized to Al (e.g. Van der Weijden, 2002). To show variability in the composition of terrigenous input through the deep marine sediments of the Zlambach Formation, we selected those elemental ratios (Ti/Al, Si/Al, Zr/Al and K/Al) which are clearly of terrigenous origin, not depending either on redox or on productivity changes. The elemental ratio of Ca/Al correlates with carbonate content (Fig. 5).

Two significant features in the lithogenic sediment fraction are clearly evident in the XRF data, showing a good correspondence to facies changes through the section. In general, the Ti/Al distribution (Fig. 5) follows the same trend as the ratios of Si/Al, Zr/Al, Ti/Al and Ca/Al through the studied interval. In detail, these ratios are consistently higher in the lower part of the section (0–29 m). In this interval, a total of ten levels (in grey, Fig. 5) with the highest values in Ti/Al, Si/Al, Zr/Al, Ca/Al and a decrease in K/Al are observed reflecting a coarsening of the facies that is also coincident with the occurrence of allodapic limestone beds (LF1-2). Shales and marls are characterised by low Ti/Al, Si/Al, Zr/Al and Ca/Al values.

4.3. Bulk carbonate C– and O–isotope stratigraphy

Carbon isotopic results from section 1 (0–33 m) reveal values that fluctuate gently around an average of 1.5‰, punctuated by a prominent shift at 33 m towards lower values down to 0.2‰ (Fig. 3). This latter negative shift can be correlated with a negative shift in the lower part of section 2 though the shift in section 2 is more progressive and stepwise and only reaches minimum values around 0.5‰ (Fig. 3a, in rectangle). The stratigraphic congruence is also supported by a good correlation for a selection of $\delta^{13}C_{carb}$ data points at the base and at the top of the overlapping interval between the two sections ($R^2 = 0.85$) (cross plot in Fig. 3). Datapoints that exhibit very negative values in section 1 have been excluded from this correlation due to potential diagenesis (Fig. 6a, see also Chapter 6.2). According to this integrated stratigraphy, a resulting composite section of the Zlambach Formation at Rossmoosgraben has been constructed by taking data from section 1 up until 33.15 m and all data of section 2 (Fig. 3).

Accordingly, the remainder of section 2 exhibits minimal values of 0.5‰ for the negative carbon isotope excursion (CIE) recorded in the *marshi* subzone between 33.5 and 41.5 m (Figs. 3, 5). This trend is followed by a 6.5 m lasting positive excursion with a sharp base and top and with values returning to an average of 1.8‰ and maximum values of 2‰ between 41.5 and 48.5 m. A second negative excursion is recorded in the last 8 m of the section with values fluctuating around 0.5‰ up until the top of the section at 56 m.

The $\delta^{18}O_{carb}$ curve (Fig. 7) shows initially negative fluctuating values between a minimum of ~−4.0 to a maximum of ~−0.5‰ in the *V. stuerzenbaumi* zone and the lower *C. marshi* zone (*C. ammonitiforme* subzone). Then, in the upper *C. marshi* zone (*C. marshi* subzone), the oxygen isotope data decrease gradually highlighting a negative trend from~−2.0‰ to ~−4.8‰ in average.

5. Micropalaeontologic results

5.1. Foraminifera

The marls and shales of the Zlambach Formation yield diverse associations of foraminifera and ostracods. The diversity and ecology of foraminifera at the Rosmoosgraben section were investigated by Weiland (1991). Typical platform foraminifera such as *Triasina* and *Aulotortus,* which were reported from calciturbidites (Matzner, 1986), were not found in the present study.

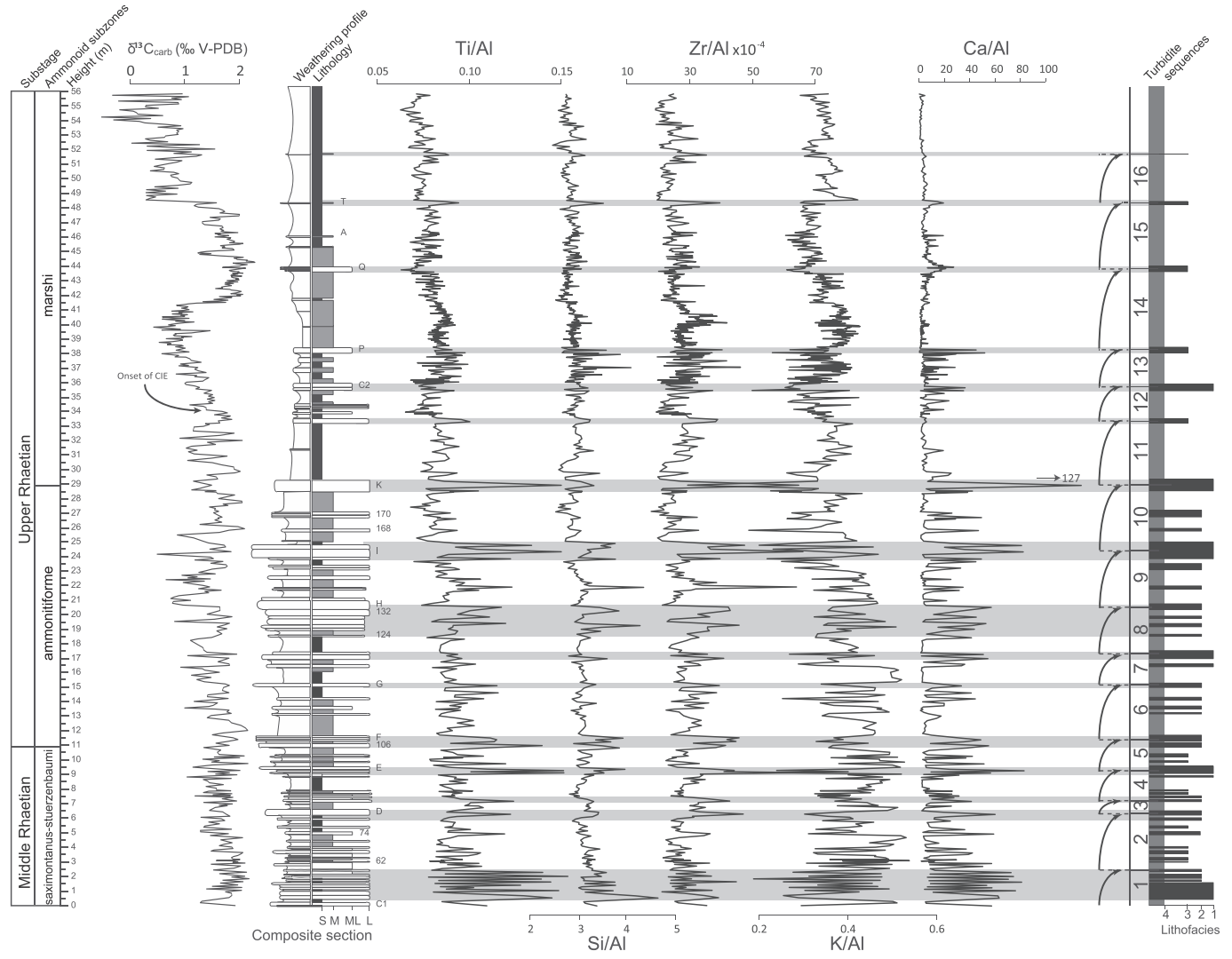

Fig. 5. Carbon isotope record and stratigraphic distribution of the main detrital proxies obtained from the Zlambach Formation at Rossmoosgraben composite section (S = shales, M = marls, ML = marly limestones, L = limestones); intervals with high Ti/Al, Si/Al and Zr/Al values are indicated by grey shading; intervals with high K/Al ratios are white.

In our material the most diverse and abundant groups are the Textulariina and Lagenina that represent autochthonous faunal elements (Weiland, 1991). The Lagenina are strongly dominated by Nodosariidae both in abundance and diversity. Oberhausellidae occur in the transgressive intervals of the section (Fig. 8) and are most frequent in the uppermost 5 m of the section. *Involutina* which was interpreted as an allochthonous faunal element (Weiland, 1991) occurs almost exclusively in the lower part of the section (below 29 m) in low to very low abundance. Relatively high abundance of *Involutina* is recorded in two samples of the uppermost 5 m of the section. The geochemical proxies for input of allochthonous sediment (Fig. 5) do not, however, indicate any sediment redeposition for this interval. Elements of other groups such as Fusulinina were only rarely found.

The foraminifera assemblages show significant variations in number of specimens and taxonomic diversity (Fig. 3). Very low diversity and abundance values occur in the upper part of the Rossmoosgraben composite section (*C. marshi* subzone) with minima at 33–34 m, 38–39 m, 44–45 m and in the uppermost 3 m of the section.

5.2. Ostracods

Ostracods from the Zlambach Formation were studied by Kollmann (1960, 1963), Bolz (1971) and Kristan-Tollmann (1970, 1971a, 1971b, 1973). These studies were, however, mainly focussed on the taxonomy of material from different sections and the palaeoecology of the ostracods is therefore still not well-known.

The present study includes a detailed quantitative, taphonomic and diversity analysis of 37 ostracod assemblages from the Rossmoosgraben section. The ostracod assemblages recovered so far from the Rossmoosgraben section include 98 species. The number of species in individual assemblages varies between 4 and 49. The Bairdioidea and Healdiidae represent >95% of the ostracod specimens, the remainder consist of Cytheroidea, Cytherellidae, Cypridida and Polycopidae.

Seven samples yielded a high number of specimens of *Ogmoconcha amphicrassa* (Kristan-Tollmann, 1971a, 1971b) and could therefore be used for a detailed age structure analysis. All these assemblages show an age structure of a low-energy thanatocoenosis according to Whatley (1988) and Boomer et al. (2003) indicating little or no post-mortem transport. All other samples with moderate specimen numbers of *O. amphicrassa* (Kristan-Tollmann, 1971a, 1971b) yielded at least a few adults and show moderate abundance of larger juveniles. A typical low-energy taphocoenosis, which indicates long-distance transport and would be expected from samples of distal turbidites, is characterised by the absence of adult specimens and strong predominance of small juveniles. Such ostracod associations were not found. The preservation of shells is good to very good and abrasive structures were rarely observed. Heavily ornamented shallow-

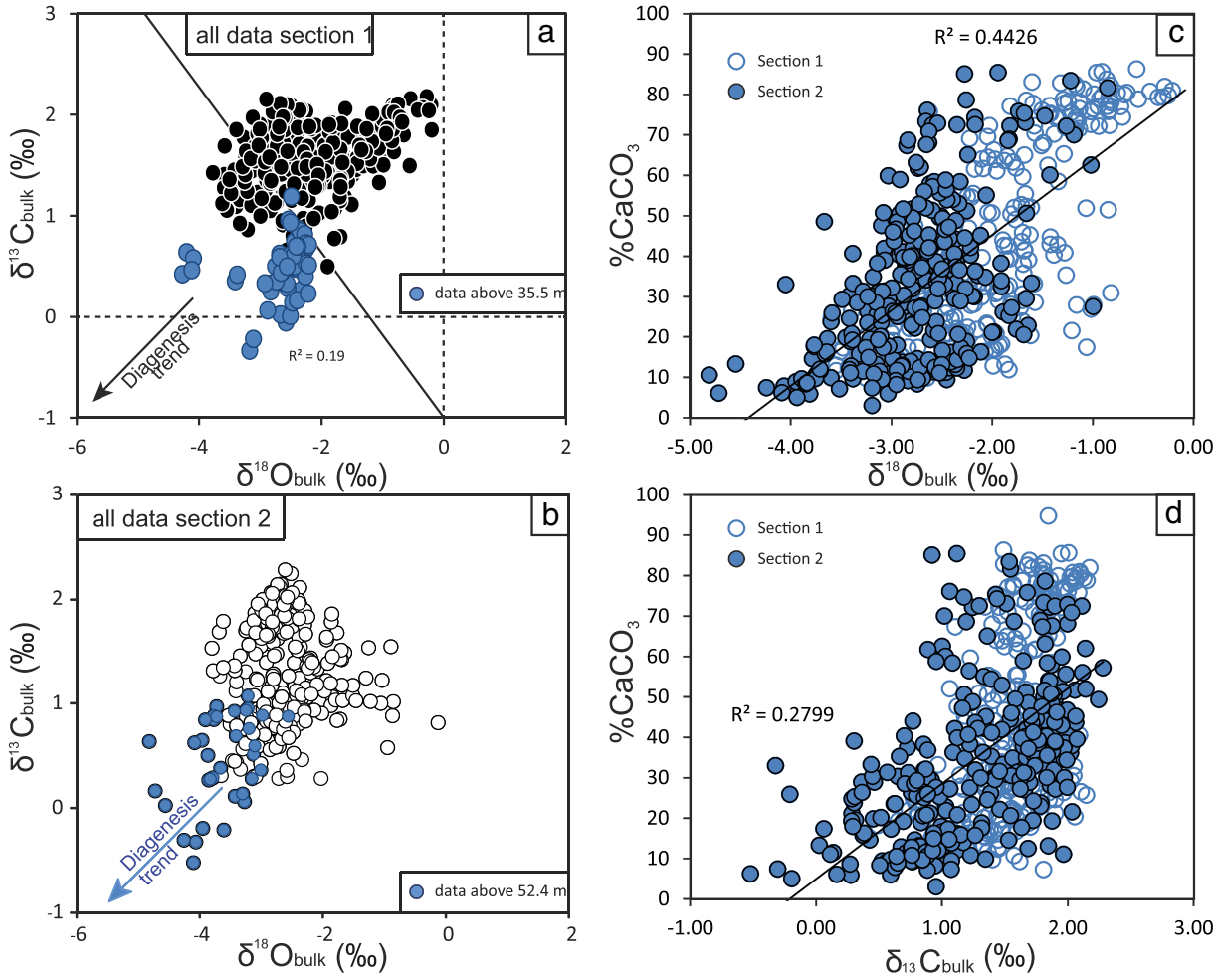

Fig. 6. (a) Cross-plot of $\delta^{13}C_{carb}$ versus $\delta^{18}O_{carb}$ (section 1); (b) Cross-plot of $\delta^{13}C_{carb}$ versus $\delta^{18}O_{carb}$ (section 2); (c) Cross-plot of % $CaCO_3$ versus $\delta^{18}O_{carb}$; (d) Cross-plot of % $CaCO_3$ versus $\delta^{13}C_{carb}$.

water taxa such as *Dicerobairdia* or *Nodobairdia* and also the shallow-water genus *Cytherelloidea* which are typical for shallow platform environments are absent or very rare.

Furthermore typical shallow platform ostracod genera like *Lutkevichinella* which was reported from the bedded Dachsteinkalk facies (Haas et al., 2007) were never found in the Zlambach beds. Other carbonate platform faunal elements which are reported from the allochthonous fossil deposits of the Fischerwiese (Matzner, 1986; Krystyn, 1991) such as coral fragments, bryozoans, calcisponges or calcareous algae are also missing or very rare in the present material.

5.2.1. Ostracod abundance and diversity

The ostracod assemblages have been analysed with respect to total and relative abundance of the taxa and ecologic diversity. The results show some significant changes both in ostracod abundance and diversity (Fig. 3). The assemblages from the lower part of the section (0–32 m) show abundances between 45 and 608 specimens and diversity values between 1.75 and 2.85 with strong variations. At 33 m the data reflect an abrupt decline to very low abundance (from 108 to 10 specimens) and diversity (Index: 2.47 to 1.03). This negative shift is followed upwards by a diversity increase at 36 m to 2.6 and another decrease at 38 m to 1.47 and low abundance (27 specimens). Another increase of diversity and abundance occurs at 41 m (172 specimens/1.95). At 45 m occurs the next minimum in abundance (6 specimens) and relative low diversity (1.5). The values increase again between 46 m and 49 m. Strong and short-term fluctuations in abundance and moderate diversity are recorded from the uppermost 3 m of the section.

Variations in ostracod and foraminifera abundance and diversity data show a remarkable coincidence with the changes of the carbon isotope curve. The first strong negative shift of ostracod abundance and diversity occurs at the same level where the first negative carbon isotope excursion starts. The interval of the negative isotope excursion (33 m to 41 m) and the subsequent positive shift (41 m to 45 m) is characterised by fluctuations between moderate and very low abundance and diversity values of the ostracods. At the top of the section (53.5 m to 56 m) occur strong short-term changes of ostracod abundance.

6. Discussion

6.1. Carbonate microfacies

The LF 1,2 and 3 represent distal calciturbiditic deposits as indicated by frequent occurrence of elements of platform origin (peloids, shallow-reef benthic foraminifera), together with typical pelagic fossil elements (radiolarians, sponge spicules and thin-shelled benthic foraminifera and ostracods). The identified shallow-water bioclasts are characteristic elements of subtidal-to-intertidal environments and are encountered in the surrounding Dachstein carbonate platform. The peloids are typical representatives of the platform, such as lagoon or open shelf environments.

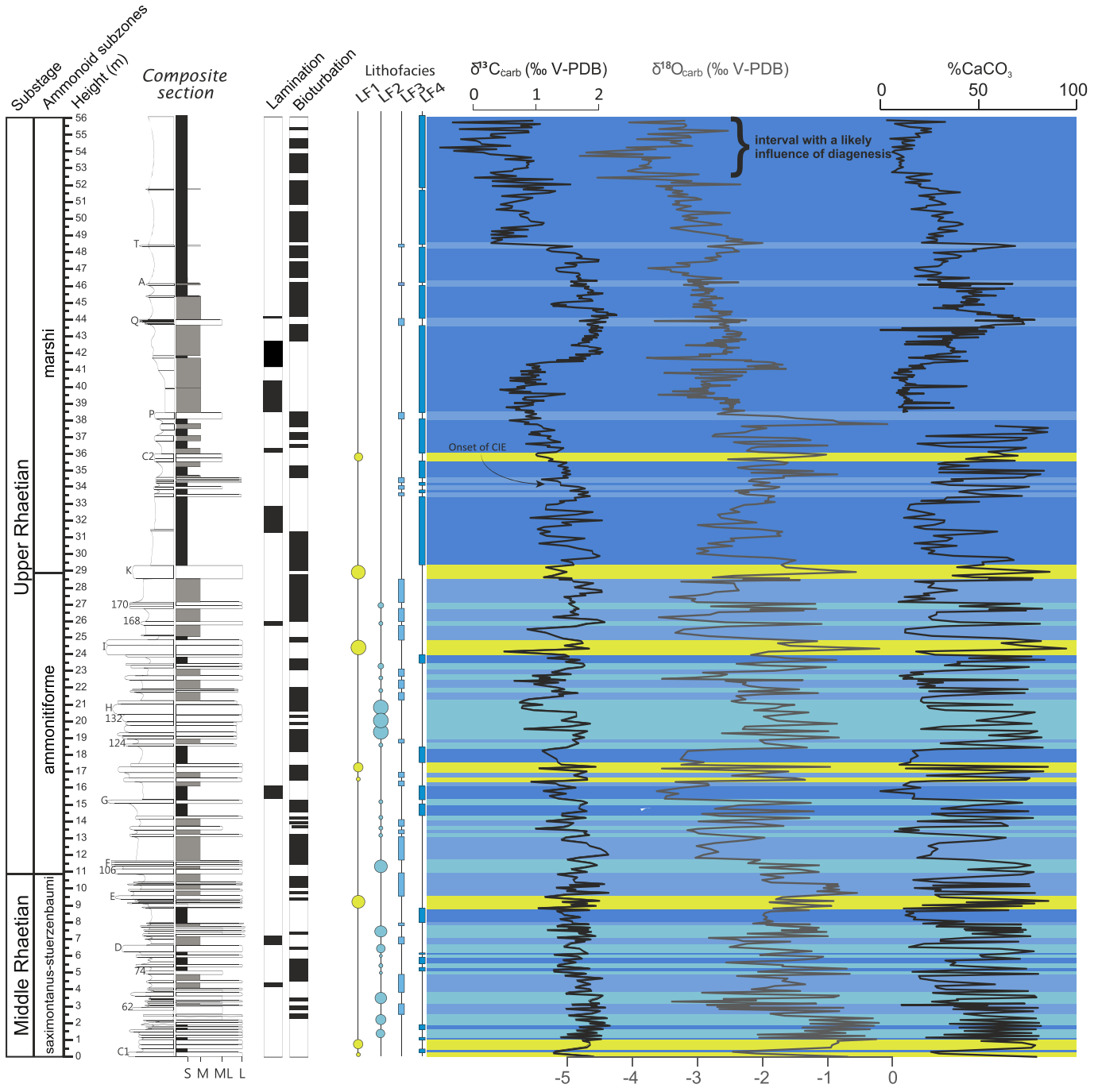

Fig. 7. Comparison of lithofacies types (LF 1-4) and sedimentary structures (lamination/bioturbation) of the Zlambach Formation at the Rossmoosgraben composite section with $\delta^{13}C_{carb}$, $\delta^{18}O_{carb}$ and $\%CaCO_3$.

Occurrence of deep-water fauna and the finer grain-size lithofacies support the distal to very distal and low density calciturbiditic nature of the resedimented limestone layers and exclude their misinterpretation as shallower tempestites. The observations of shallow-water fauna also distinguish the studied calciturbidite deposits from bottom current deposits. This finding is supported by the absence of grains with iron staining or ferro-manganese coatings observed in contourites. The poor sorting of the lithofacies in medium-grained sequences is an additional typical feature of calciturbidites. The sedimentologic features and fossil assemblages of the Zlambach Formation thus point to a distal toe–of–slope depositional environment, in the slope to basin transitional zone (Table 1) which is in concert with earlier sedimentologic studies of the Zlambach Formation (Matzner, 1986).

The lithology and interpretation of microfacies, as well as the biostratigraphy of the Rossmoosgraben section, which exposes the middle and upper Rhaetian of the Zlambach Formation, are shown in Fig. 4. Calciturbidite is the most characteristic facies in the lower part of the section (0–29 m; *V. stuerzenbaumi* zone and *C. ammonitiforme* subzone) followed by predominant pelagic deposits in the *C. marshi* subzone (29–56 m). The calciturbidites display m-scale coarsening upward sequences with medium (LF1, LF2) and fine-grained (LF3, LF4) intervals, representing well-distinguished sedimentary layers. The resedimented limestones become thicker and bioturbated upwards and the most prominent calciturbidite bed K (Figs. 3, 4) marks the transition between the calciturbidite-dominated deposits of the lower section and pelagic deposits of the upper part of the section.

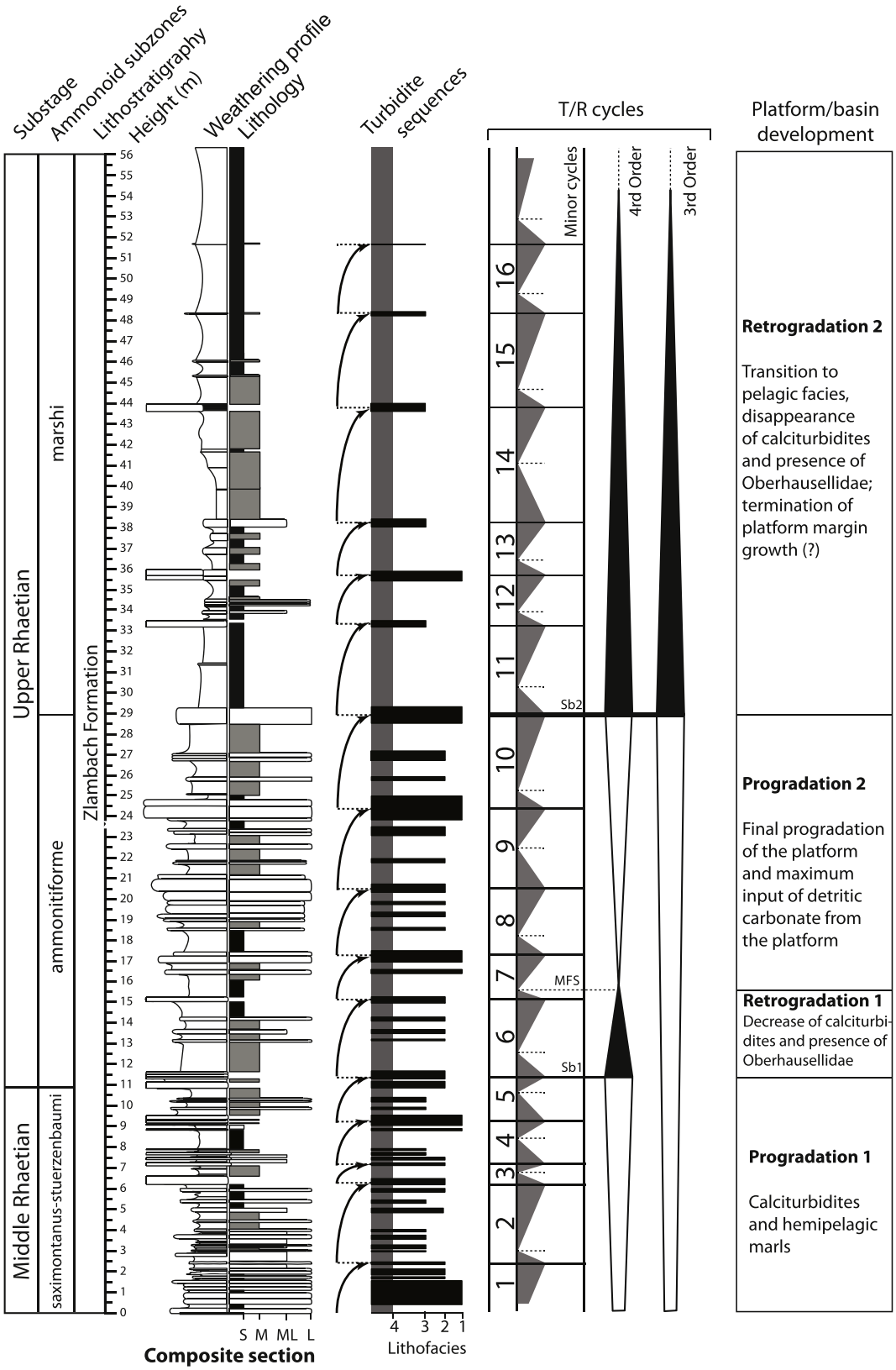

Fig. 8. Lithostratigraphy, calciturbidites, T/R cycles, occurrence of Oberhausellidae (*) at the Rossmoosgraben composite section and inferred platform/basin development (S = shale, M = marl, ML = marly limestone, L = limestone).

6.2. Geochemical results

The geochemical trends observed in the lower part of the section, from 0 to 29 m (Fig. 5), reflect ten levels showing a coarsening of the facies and a strong increase of Ti/Al, Si/Al, Zr/Al and Ca/Al ratios that is coincident with the occurrence of calciturbidites (LF1-2). The positive peaks of Ti/Al, Si/Al, Zr/Al and Ca/Al ratios (Fig. 5) indicate maxima in fluvial sediment input.

These latter previously interpreted as the basal part of turbiditic sequences are followed by a rise in K/Al values, whereupon the facies becomes finer grained mudstones. Minima in Ti/Al, Si/Al, Zr/Al and Ca/Al values are reached in coincidence with the change to pelagic deposits (LF4) above 29 m, with six intercalated distal turbidites (LF3; Fig. 5).

Regional patterns of variation in terrigenous proxy records can provide information about sources and fluxes of detrital material within the Hallstatt Basin. These changes are broadly aligned with facies changes. The calciturbidites present a stacking architecture that allows drawing stratigraphic sequences (Fig. 8). This sequence stratigraphic feature is typically used to recognise patterns in relative sea-level change (De Graciansky et al., 1998; Church and Coe, 2003).

6.2.1. Carbon isotope record

The carbon isotope record preserved in the marine rock record ($\delta^{13}C_{carb}$) is strongly depending on the partitioning between the marine carbonate carbon and organic pools (e.g. Scholle and Arthur, 1980; Weissert, 1989). Whereas positive shifts in the $\delta^{13}C_{carb}$ are generally related to enhanced marine burial of sedimentary organic relative to inorganic carbon (Jenkyns, 2010), negative CIEs might be related to reduced organic productivity, diminished organic carbon burial or processes remobilizing ^{13}C depleted carbon such as volcanism or methane hydrate release (e.g. Menegatti et al., 1998; Hesselbo et al., 2002; Tanner, 2010). Shallow water carbonate sediments deposited in situ are not reliable recorders of global $\delta^{13}C_{carb}$ as they are known to be affected by short-term changes in sea level, which subject the deposits to influences of meteoric diagenesis during which time the $\delta^{13}C_{carb}$ can be altered substantially (Swart, 2008). A more diagenetically stable environment is found on the slopes of carbonate platforms, at depths below sea-level changes, where mixtures of pelagic and platform-derived sediments are deposited. In these location the $\delta^{13}C_{carb}$ of carbonate sediments, although subjected to closed-system diagenesis, are not substantially altered from their original $\delta^{13}C_{carb}$ values.

In the present study, the cross-plot of all carbon and oxygen isotope data of bulk samples from Rossmoosgraben (Fig. 6a) reveal a low covariance between $\delta^{13}C_{carb}$ and $\delta^{18}O_{carb}$ ($R^2 = 0.19$) suggesting that a diagenic impact, at least for one of the isotope systems, is only minor. A number of data points of section 1 appeared to stand out of the cloud with more negative values in both isotopic systems but particularly in $\delta^{13}C$ (Fig. 6a). These values corresponding to the very pronounced negative excursion expressed in section 1 above 35.5 m (Fig. 3), we did not take them into account in our composite and preferred values of section 2 for this stratigraphic interval. The cross-plot between $\delta^{18}O$ and $\delta^{13}C$ of section 2 also appears to highlight potential alteration for values above 52.4 m (Fig. 6b). This is also in concert with the stronger fluctuating $\delta^{13}C$ values at this stratigraphic level, a feature that is often caused by intermittent diagenetic impacts. Diagenesis, however, appears insufficient to explain the two $\delta^{13}C$ negative excursions of the *marshi* zone.

We also note that high-frequency fluctuations are more common in the lower part of the Rossmoosgraben $\delta^{13}C_{carb}$ record (0–29 m), suggesting alteration of the primary carbon-isotope signature within calciturbiditic sequences characterised by significant increased detrital fraction (Fig. 7). The regressive phases in this stratigraphic interval have substantially superimposed the effect of diagenetic processes on the carbonates such as ^{13}C-depleted cements (Allan and Matthews, 1982; Joachimski, 1994; Sattler et al., 2005; Immenhauser et al., 2008). Moreover, the carbon isotopic composition of our carbonates fall in the range of 2.3‰ to ~0.5‰ minimum, typical for pelagic and hemipelagic records (e.g., Jarvis et al., 2001; Muttoni et al., 2014).

The $\delta^{18}O_{carb}$ values show strong fluctuations in relation to lithofacies changes. Lighter $\delta^{18}O_{carb}$ values characterise marly beds, whereas heavier $\delta^{18}O_{carb}$ values are related to limestone beds, and this is well-reflected in the correlation between $\%CaCO_3$ and $\delta^{18}O_{carb}$ (Fig. 6c) We also note that a slightly less significant correlation can also be observed between $\%CaCO_3$ and $\delta^{13}C_{carb}$ (Fig. 6d). These observations could reflect a reduced diagenetic impact in calciturbidites (Fig. 7).

6.2.2. Comparison with other Middle to Late Rhaetian $\delta^{13}C_{carb}$ records

As stated in the introduction there is presently no other high-resolution C_{carb} record of the Middle-Late Rhaetian interval which could be directly compared with the present data. The Rhaetian C_{carb} curve of the sections in the southern Alps of northern Italy (Muttoni et al., 2014) shows strong fluctuations. They found oscillations of 3‰ in C_{carb} at the Italcementi quarry section and 3‰ in C_{carb} respectively at the Brumano section. These strong variations were explained by the latter authors by mixing of shallow water carbonates from different sources. Although no statistical analysis of carbon and oxygen isotope data were provided the latter authors stated that these isotope data would represent original signals. Moreover the Rhaetian sections in the Southern Alps are not dated biostratigraphically due to the lack of ammonites and conodonts and the isotope record is therefore not comparable with the present data. Another C_{carb} record was reported from Rhaetian sediments at the Pignola-Abriola section in southern Italy (Rigo et al., 2015) which were deposited in the deep marine Lagonegro Basin. This isotope record is of at least ten times lower stratigraphic resolution and focussing on the Norian-Rhaetian boundary and not the Middle Rhaetian. It is also not clear if these data were affected by diagenesis as statistical analysis of the isotope data is lacking. The $\delta^{13}C_{carb}$ data in Rigo et al. (2015) are thus also not directly comparable with the present isotope results. In contrast to the present results the $\delta^{13}C_{carb}$ curve in Rigo et al. (2015) shows several minor fluctuations of 1‰ $\delta^{13}C_{carb}$ or less and a long-term positive trend throughout the Rhaetian. Therefore a direct comparison of the $\delta^{13}C_{carb}$ curve from southern Italy with the present results is not possible.

The carbon isotope trend of Zaffani et al. (2018) for Northern Italy is based on bulk organic matter. A negative excursion is observed in the middle of the Rhaetian and this was correlated by these authors with a negative wiggle of the low resolution dataset of Whiteside and Ward (2011) provided for British Columbia. The biostratigraphic control, however, is poor. Because of both, the low resolution of the data and the poor biostratigraphic control of the literature dataset(s), it is difficult to correlate these isotope trends with our negative carbon isotope excursion. The stratigraphic part of the negative $\delta^{13}C$ excursion(s) in the lower part of the Rhaetian presented by Zaffani et al. (2018) is not covered in our record.

6.3. Establishing a sequence stratigraphic framework for the Rossmoosgraben deposits

The facies characteristics of the succession exposed in Rossmoosgraben suggest a long–term deepening trend in the early Rhaetian to early Hettangian interval which was related to the opening of the western ("Ligurian") Tethys and corresponds to the so-called "Rhaetian" transgression of central Europe (De Graciansky et al., 1998; Hallam, 2001) establishing marine connections between the Tethyan and Boreal oceans along the proto–Atlantic seaway.

The lithofacies and geochemical proxies have revealed the presence of numerous calciturbidites that present a stacking architecture with sequences of carbonate beds that become progressively thicker (Fig. 8). Turbid flows are the result of slope instability and therefore, the most likely explanation for such sequences is that of a sea-level control. Accordingly, a medium, third-order (sensu De Graciansky et al., 1998) regressive–transgressive sea level cycle is known to have occurred from the *V. stuerzenbaumi* zone to *C. marshi* zone. At the base of the transgressive tract, a sequence boundary (SB2) records the abrupt change in lithology from the predominance of calciturbidites to more pelagic facies.

The base of each fourth-order cycle is delineated by sequence boundaries (SB 1, SB 2) and reflected by maxima in the Ti/Al, Si/Al and Zr/Al values (coarse detrital fraction, see Fig. 5), whereas the end of the transgression, represented by a maximum flooding surface (MFS) corresponds

to the highest relative proportion of the K/Al ratio (fine detrital fraction). The lowest part of the section (*V. stuerzenbaumi* zone) corresponds to the end of the regression of cycle 1 and terminates at 11 m.

The stratigraphic episodes of elevated K/Al ratios (Fig. 5) of the 16 "low-order" or minor cycles can be explained either by changes in the contribution of clay minerals or by changing ratios of fluvial versus aeolian sediment supply due to rapid sea-level changes and/or rapid, possibly orbital climatic variations that influenced sediment supply and loading on the slope. Within the 16 "low-order" or minor cycles, levels attributed to aeolian dust plumes are dominant at the base of each cycle whereas components transported by fluvial input are dominant at the top of each cycle.

6.4. Discussion of micropalaeontological results

The taphonomic analysis and taxonomic composition of the microfossil assemblages suggest that they were not significantly affected by redeposition. Therefore the suggestion of Krystyn (1991) and Richoz and Krystyn (2015) that the microbenthic assemblages from marly beds of the Zlambach Formation were generally transported from the Dachstein platform has to be rejected. According to the results of the microfacies and XRF analysis sediment redeposition from the platform was largely confined to the carbonate beds (see Chapters 4.2. and 6.2.).

According to Weiland (1991) the foraminifera suggest a predominance of favourable environmental conditions which were interrupted by short intervals of high organic input and low oxygen concentrations indicated in the lowermost part of the section and above 29 m by the predominance of infaunal taxa. The foraminifera associations from the upper part of the section (above 29 m) were interpreted to reflect alternations between normal and low oxygen conditions (Weiland, 1991). The predominance of nodosariid foraminifera in the present material is in accordance with a deep neritic environment. The relatively high abundance of Oberhausellidae at the top of the section may be either due to great water depths or short periods of oxygen deficiency (Clemence and v. Hillebrandt, 2013). A detailed palaeoecologic analysis of foraminifera from the upper part of the section (above 29 m) (Konrad, 2014) demonstrated a significant drop in diversity at 41–45 m where the positive carbon isotope excursion occurs (Figs. 2, 4) indicating stressed environmental conditions. The high species diversity of the ostracods and absence of deep-water as well as typical shallow-water taxa is also suggestive of a deep neritic environment.

There is a coincidence between the first negative carbon isotope excursion and the decrease in ostracod and foraminifera abundance and diversity at the base of section 2, around 33.5 m as well as strong fluctuations in the abundance and diversity of ostracods and foraminifera in the intervals 34–45 m and 52–56 m (Fig. 3) that suggests an environmental perturbation in the *C. marshi* ammonoid subzone.

In summary most ostracod and foraminifera associations of the Rossmoosgraben section were not affected by redeposition and they reflect a predominance of stable and favourable conditions at the sea floor during the middle Rhaetian (*V. stuerzenbaumi* zone) and early late Rhaetian (lower *C. marshi* zone; *C. ammonitifome* subzone). For the upper *C. marshi* zone the benthic microfossil data are indicative of significant environmental deterioration.

6.5. Basin development

The basin development is summarized in Fig. 8. The middle and upper Rhaetian succession encountered in the Rossmoosgraben section shows a regressive-transgressive trend. The lower part of the section (0–29 m; *V. stuerzenbaumi* zone, *C. ammonitiforme* subzone), shows a predominance of distal toe–of–slope facies. The lower part of this interval (0–11.5 m) represents a first phase of platform progradation which is followed upwards (11.5–15.5 m) by a retrogradation as indicated by the decrease of calciturbidites and first occurrence of deep-water foraminifera (Oberhausellidae). The interval between 15.5 m and 29 m shows an upward increasing input of detrital carbonate reflecting a second platform progradation. In the upper part of the section (29–56 m; *C. marshi* subzone) calciturbiditic beds become successively thinner and much less frequent indicating platform retrogradation. The uppermost 8 m of the section are devoid of any calciturbidite which may be either due to increasing distance of the source area or to a final cessation of platform margin growth.

Krystyn et al. (1991) suggested a drowning of the Dachstein reef and platform margin during the middle Rhaetian (*V. stuerzenbaumi* zone). The sequence stratigraphic results and occurrence of abundant and thick calciturbidites with platform derived components in the lower part of the Rossmoosgraben section (Fig. 8), however, suggest that the platform margin growth continued at least until the late Rhaetian (lower *C. marshi* zone, *C. ammonitiforme* subzone).

Our results also show a stratigraphic coincidence of significant carbon isotope excursions, rapid depletion of ostracod and foraminifera abundance and diversity and the disappearance of calciturbidites. This coincidence may be purely accidental. In our view this interpretation seems however improbable. We suggest a causal link of the sedimentological, micropalaeontological and geochemical changes reflecting an environmental perturbation and ecological change in the Hallstatt facies zone. In our view the most plausible interpretation is that this change was related to the cessation of the Dachstein platform margin growth. We are aware that this interpretation has to be confirmed by further extensive research in particular with regard to the biostratigraphy of the Dachstein platform and reef carbonates.

Within this framework of long–term facies changes, short–term facies changes can also be seen which may reflect minor sea–level or orbital climatic changes. The 16 "low order" cycles show microfacies types LF1 and 2 at the top with a high amount of platform-derived microfossils and peloids indicative of highstand-shedding intervals (Reijmer et al., 1992; Schlager et al., 1994). The stacking pattern of these cycles would be consistent with a control by Milankovitch periodicities (pers. comm. J. Pálfy). Shoaling upward cycles are a general feature of the Dachstein platform development. The famous Norian "Lofer cycles" were originally interpretated as deepening—upward units (Fischer, 1975) but later studies came to the conclusion that they were predominantly affected by periodic sea level drops (Goldhammer et al., 1990; Satterley, 1996; Enos and Samankassou, 1998; Haas et al., 2007). Minor sea level oscillations with short-term platform exposure of the Dachstein platform were also recorded by variations in turbidite composition of the upper Norian Pedatakalk Formation and the Pötschenkalk Formation of the NCA (Reijmer and Everaars, 1991; Reijmer et al., 1994). A shallowing—upward calciturbidite cyclicity, similar to that observed in the Zlambach Formation, was reported from Rhaetian basinal deposits of the Lombardy Basin in the southern Alps (Burchell et al., 1990). Transgressive-regressive cycles in late Rhaetian intraplatform basin deposits (Kössen Formation) also reflect periodic sea level drops (Golebiowski, 1989; Holstein, 2004) as highlighted by gamma ray spectroscopy results (Mette et al., 2016). Although Milankovitch periodicities were identified in Late Triassic calciturbidites of the Pedatakalk and Pötschenkalk Formations (e.g. Goldhammer et al., 1990; Reijmer et al., 1994) other factors such as tectonic control or autocyclic processes were also suggested (e.g. Goldhammer et al., 1990; Satterley and Brandner, 1995; Satterley, 1996) to play an important role for the cyclicity in Late Triassic platform deposits of the Alps.

A water depth of at least 300–500 m or even deeper has been estimated for the Hallstatt Basin during the Norian by Kenter and Schlager (2009) based on the geometry of clinoforms at the Dachstein carbonate platform slope. The latter authors stated, however, that the water depth may have decreased significantly during the Rhaetian due to terrigenous input in the Hallstatt Basin and may have also been changed by syndepositional movements between the platform and the basin. The benthic microfossil assemblages indicate that the depositional depth of the Zlambach Formation was probably not >300 m

because typical bathyal ostracod genera with long spines such as *Acanthoscapha* or *Nemoceratina*, are absent or very rare. The high species diversity (at least 98 species) of the ostracod fauna would also be in better accordance with deep subtidal conditions than with a bathyal environment (Benson, 1988).

7. Conclusions

The Zlambach Formation exposed at Rossmoosgraben section is an open marine regressive-transgressive succession of marl-limestone alternations which was deposited in a toe—of—slope to basin environment and ranges in age from Middle to Late Rhaetian.

Sequence boundaries, transgressive surfaces and maximum flooding surfaces of 3rd and 4th order sequences and related to long-term sea level changes are recorded by detrital proxies indicating maxima and minima of terrestrial sediment input and by abrupt changes in the input of detrital carbonate from the platform. Minor sea level fluctuations are indicated by subordinate coarsening— and thickening—upward cycles characterised by distal calciturbidites which were derived from the Dachstein carbonate platform and slope.

The occurrence of platform derived calciturbidites in the late Rhaetian (*C. marshi* zone) is in contrast to the results of earlier studies indicating a drowning and cessation of Dachstein reef and platform margin growth during the middle Rhaetian (*V. stuerzenbaumi* zone). The present results are indicative of a final cessation of platform margin growth during the upper *C. marshi* zone.

Carbon isotope data of the Rossmoosgraben section show a 1.0‰ negative excursion and a subsequent 1.3‰ positive excursion in the upper *C. marshi* zone which is followed upwards by another gradual negative trend towards the top of the section. These results suggest that significant changes in carbon isotope ratios in the late Rhaetian were not confined to the intraplatform environments (Mette et al., 2012; Korte et al., 2017) but occurred as well in the open marine realm of the western Tethys.

The micropalaeontogical results show significant changes in abundance and diversity of ostracods and foraminifera in stratigraphic coincidence with the carbon isotope excursions in the upper Zlambach Formation (upper *C. marshi* zone) suggesting some important perturbations of marine environments in the western Tethys during the late Rhaetian.

The stratigraphic coincidence between the carbon isotope excursions, impoverishment of benthic fossils associations and the disappearance of calciturbidites suggests a causal link with the termination of the Dachstein platform margin reef growth.

Acknowledgements

The help of Sergio Salvemini during fieldwork and the laboratory work of Parvin Mohtat-Aghai and Maria Schaffhauser are kindly acknowledged. Leo Krystyn (University of Vienna) kindly determined the ammonoids. Sylvain Richoz (University of Lund) is thanked for discussions and cooperation during the fieldwork. We thank also Myriam Boussaha (University of Copenhagen) for trace fossil determinations. The research was financed by the Austrian Science Fund (FWF) (Project 25782).

References

Ahm, A.-S., Bjerrum, C.J., Hammarlund, E.U., 2017. Disentangling the record of diagenesis, local redox conditions, and global seawater chemistry during the latest Ordovician glaciation. Earth and Planetary Science Letters 459, 145–156. https://doi.org/10.1016/j.epsl.2016.09.049.

Allan, J.R., Matthews, R.K., 1982. Isotope signatures associated with early meteoric diagenesis. Sedimentology 29, 797–817.

Benson, R.H., 1988. Ostracods and palaeoceanography. In: De Deckker, P., Colin, P., Peypouquet, J.P. (Eds.), Ostracoda in the Earth Sciences. Elsevier, Amsterdam, pp. 1–26.

Bolz, H., 1971. Die Zlambach-Schichten (alpine Obertrias) unter besonderer Berücksichtigung der Ostrakoden. Senckenbergiana Lethaea 52 (2/3), 129–283.

Boomer, I., Horne, D.J., Slipper, I.J., 2003. The use of ostracods in palaeoenvironmental studies, or what you can do with an ostracod shell? In: Park, L., Smith, A.J. (Eds.), Bridging the Gap – Trends in the Ostracode Biological and Geological Sciences. Paleontological Society Papers 9, pp. 153–173

Burchell, M.T., Stefani, M., Masetti, D., 1990. Cyclic sedimentation in the Southern Alpine Rhaetic: the importance of climate and eustasy in controlling platform-basin interactions. Sedimentology 37, 795–815.

Church, K.D., Coe, A.L., 2003. Processes controlling relative sea-level change and sedimentary supply. In: Coe, A.L. (Ed.), The Sedimentary record of sea level change. Cambridge University Press, pp. 99–117.

Clemence, M.-E., v. Hillebrandt, A., 2013. Oberhausellidae (Benthic Foraminifera) outbursts during the environmental perturbations at the Triassic-Jurassic boundary: Palaeoecological Implications. In: Georgescu, M.D. (Ed.), Foraminifera: Aspects of Classification. Nova Science Publishers, Stratigraphy, Ecology and Evolution, pp. 1–20.

Dahl, T.W., Ruhl, M., Hammarlund, E.U., Canfield, D.E., Rosing, M.T., Bjerrum, C.J., 2013. Tracing euxinia by molybdenum concentrations in sediments using handheld X-ray fluorescence spectroscopy (HHXRF). Chemical Geology 360-361, 241–251.

De Graciansky, P.C., Jacquin, T., Hesselbo, S.P., 1998. The Ligurian cycle: an overview of Lower Jurassic 2nd order transgressive-regressive facies cycles in western Europe. In: de Graciansky, P.C., Hardenbol, J., Jaquin, T., Vail, P.R. (Eds.), Mesozoic and Cenozoic Sequence Stratigraphy of European Basins. SEPM Special Publication Series No. 60. SEPM (Society for Sedimentary Geology), Tulsa (786 pp.).

Dunham, R.J., 1962. Classification of carbonate rocks according to depositional texture. American Association of Petroleum Geologists Memoirs 1, 108–121.

Enos, P., Samankassou, E., 1998. Lofer cycles revisited (late Triassic, Northern Alps, Austria). Facies 38, 207–228.

Felber, R., Weissert, H.J., Furrer, H., Bontognali, T.R.R., 2015. The Triassic-Jurassic boundary in the shallow water marine carbonates from the western Northern Calcareous Alps. Swiss Journal of Geosciences 108, 213–224.

Fischer, A.G., 1975. Tidal deposits, Dachstein limestone of the North-Alpine Triassic. In: Ginsburg, R.N. (Ed.), Tidal Deposits: A Casebook of Recent Examples and Fossil Counterparts. Springer, Berlin, Heidelberg, New York, pp. 234–242.

Flügel, E., 2004. Microfacies of Carbonate Rocks. Springer-Verlag, Berlin-Heidelberg.

Folk, R.A., 1959. Practical petrographic classification of limestones. Bulletin of the American Association of Petroleum Geologists 43, 1–38.

Goldhammer, R.K., Dunn, P.A., Hardie, L.A., 1990. Depositional cycles, composite sea-level changes, cycle stacking patterns, and the hierarchy of stratigraphic forcing: examples from the Alpine Triassic platform carbonates. Geological Society of America Bulletin 102, 535–562.

Golebiowski, R., 1989. Stratigraphie und Biofazies der Kössener Formation (Obertrias, Nördliche Kalkalpen). Ph.D. Thesis (unpubl.). University of Vienna.

Grabau, A.W., 1904. On the classification of sedimentary rocks. American Geology 33, 228–247.

Haas, J., Lobitzer, H., Monostori, M., 2007. Characteristics of the Lofer cyclicity in the type locality of the Dachstein Limestone (Dachstein Plateau, Austria). Facies 53, 113–126.

Haas, J., Götz, A.E., Pálfy, J., 2010. Late Triassic to Early Jurassic Palaeogeography and Eustatic History in the NW Tethyan Realm: New Insights from Sedimentary and Organic Facies of the Csővár Basin (Hungary). Palaeogeography, Palaeoclimatology, Palaeoecology 291, 456–468.

Hallam, A., 2001. A review of the broad pattern of Jurassic sea-level changes and their possible causes in the light of current knowledge. Palaeogeography, Palaeoclimatology, Palaeoecology 167, 2–37.

Hesselbo, S.P., Robinson, S.A., Surlyk, F., Piasecki, S., 2002. Terrestrial and marine extinction at the Triassic-Jurassic boundary synchronized with major carbon-cycle perturbation: a link to initiation of massive volcanism? Geology 30, 251–254.

Holstein, B., 2004. Palynologische Untersuchungen der Kössener Schichten (Rhät, Obertrias). Jahrbuch der Geologischen Bundesanstalt 144 (3/4), 261–365.

Hornung, T., Brandner, R., Krystyn, L., Joachimski, M., Keim, L., 2008. Multistratigraphic constraints of the NW Tethyan "Carnian Crisis". In: Lucas, S.G., Spielmann, J.A. (Eds.), The Global Triassic. New Mexico Museum of Natural History and Science Bulletin 41, pp. 59–67.

Immenhauser, A., Holmden, C., Patterson, W.P., 2008. Interpreting the carbon-isotope record of ancient shallow Epeiric Seas: lessons from the recent. Geological Association of Canada Special Paper 48 (4), 137–174.

Jarvis, I., Murphy, A.M., Gale, A.S., 2001. Geochemistry of pelagic and hemipelagic carbonates: criteria for identifying systems tracts and sea-level change. Journal of the Geological Society, London 158, 685–696.

Jenkyns, H.C., 2010. Geochemistry of oceanic anoxic events. Geochemistry, Geophysics, Geosystems 11 (3), 1–30.

Joachimski, M., 1994. Subaerial exposure and deposition of shallowing upward sequences: evidence from stable isotopes of Purbeckian peritidal carbonates (basal cretaceous), Swiss and French Jura Mountains. Sedimentology 41 (4), 805–824.

Kenter, J.A.M., Schlager, W., 2009. Slope angle and basin depth of the Triassic platform-basin transition at the Gosaukamm, Austria. Austrian Journal of Earth Science 102, 15–22.

Kollmann, K., 1960. Ostracoden aus der alpinen Trias Österreichs. I. *Parabairdia* n.g. und *Ptychobairdia* n.g. (Bairdiidae). Jahrbuch der Geologischen Bundesanstalt, Sonderband 5, 79–105.

Kollmann, K., 1963. Ostracoden aus der alpinen Trias. II. Weitere Bairdiidae. Jahrbuch der Geologischen Bundesanstalt 106 (1), 121–203.

Konrad, B., 2014. Ecological Patterns of Benthic Foraminifera in Response to Upper Triassic Environmental Changes: From the Zlambach Schichten, Northern Calcareous Alps, Austria. Bachelor Thesis. University of Innsbruck (unpublished).

Korte, C., Kozur, H., 2011. Bio- and chemostratigraphic assessment of carbon isotopes records across the Triassic-Jurassic boundary at Csövár quarry (Hungary) and Kendlbachgraben (Austria) and implications for global correlations. Bulletin of the Geological Society of Denmark 59, 101–115.

Korte, C., Kozur, H.W., Veizer, J., 2005. $\delta^{13}C$ and $\delta^{18}O$ values of Triassic brachiopods and carbonate rocks as proxies for coeval seawater and palaeotemperature. Palaeogeography, Palaeoclimatology, Palaeoecology 226 (3–4), 287–306. https://doi.org/10.1016/j.palaeo.2005.05.018.

Korte, C., Thibault, N., Ullmann, C.V., Clemence, M.-E., Mette, W., Olsen, T.K., Rizzi, M., Ruhl, M., 2017. Brachiopod biogeochemistry and isotope stratigraphy from the Rhaetian Eiberg section in Austria: potential and limitations. Neues Jahrbuch für Geologie und Paläontologie 284 (2), 117–138.

Korte, C., Ruhl, M., Pálfy, J., Ullmann, C.V., Hesselbo, S.P., 2019. Chemostratigraphy across the Triassic–Jurassic boundary. In: Sial, A.N., Gaucher, C., Ramkumar, M., Ferreira, V.P. (Eds.), Chemostratigraphy Across Major Chronological Boundaries. Geophysical Monograph 240, pp. 185–210.

Kristan-Tollmann, E., 1970. Einige neue Bairdien (Ostracoda) aus der alpinen Trias. Neues Jahrbuch für Geologie und Paläontologie, Abhandlungen 135 (3), 268–310.

Kristan-Tollmann, E., 1971a. *Torohealdia* n.g., eine charakteristische Ostracoden-Gattung der obersten alpinen Trias. Erdoel-Erdgas-Zeitschrift 87, 49–54.

Kristan-Tollmann, E., 1971b. Zur phylogenetischen und stratigraphischen Stellung der triadischen Healdiiden (Ostracoda). Erdoel-Erdgas-Zeitschrift 87, 428–438.

Kristan-Tollmann, E., 1973. Zur phylogenetischen und stratigraphischen Stellung der triadischen Healdiiden (Ostracoda). II. Erdoel-Erdgas-Zeitschrift 89, 150–155.

Krystyn, L., 1987. Zur Rhät-Stratigraphie in den Zlambach-Schichten (vorläufiger Bericht). Österreichische Akademie der Wissenschaften, Sitzungsberichte der Mathematisch-Naturwissenschaftlichen Klasse, Abteilung 1 196 (3), 21–36.

Krystyn, L., 1990. A Rhaetian stage – chronostratigraphy, subdivisions and their intercontinental correlation. Albertiana 8, 15–24.

Krystyn, L., 1991. Die Fossillagerstätten der alpinen Trias. In: Nagel, D., Rabeder, G. (Eds.), Exkursionen im Jungpaläozoikum und Mesozoikum Österreichs. Österreichische Paläontologische Gesellschaft, Wien, pp. 23–78.

Krystyn, L., Mandl, G.W., Schauer, M., 1991. Growth and termination of the Upper Triassic platform margin of the Dachstein area (Northern Calcareous Alps). Austrian Journal of Earth Sciences 102, 23–33.

Kürschner, W.M., Bonis, N.R., Krystyn, L., 2007. Carbon-isotope stratigraphy and palynostratigraphy of the Triassic–Jurassic transition in the Tiefengraben section—Northern Calcareous Alps (Austria). Palaeogeography, Palaeoclimatology, Palaeoecology 244, 257–280.

Mandl, G.W., 2000. The Alpine sector of the Tethyan shelf – examples of Triassic to Jurassic sedimentation and deformation from the Northern Calcareous Alps. Mitteilungen der Österreichischen Geologischen Gesellschaft 92 (1999), 61–77.

Maslo, M., 2008. Taxonomy and stratigraphy of the Upper Triassic heteromorphic ammonoids: preliminary results from Austria. Berichte der Geologischen Bundesanstalt 76, 15–16.

Matzner, C., 1986. Die Zlambach-Schichten (Rhät) in den Nördlichen Kalkalpen: Eine Plattform-Hang-Beckenentwicklung mit allochthoner Karbonatsedimentation. Facies 14, 1–104.

Menegatti, A.P., Weissert, H., Brown, R.S., Tyson, R.V., Farrimond, P., Strasser, A., Caron, M., 1998. High resolution $\delta^{13}C$ stratigraphy through the early Aptian "Livello Selli" of the Alpine Tethys. Paleoceanography 13 (5), 530–545.

Mette, W., Elsler, A., Korte, C., 2012. Palaeoenvironmental changes in the Late Triassic (Rhaetian) of the Northern Calcareous Alps: clues from stable isotopes and microfossils. Palaeogeography, Palaeoclimatology, Palaeoecology 350–352, 62–72.

Mette, W., Thibault, N., Krystyn, L., Korte, C., Clemence, M.-E., Rizzi, M., Ullmann, C.V., 2016. Field trip 11: Rhaetian (late Triassic) biotic and carbon isotope events and intraplatform basin development in the Northern Calcareous Alps, Tyrol, Austria. Geology of the Alps 13, 233–257.

Muttoni, G., Mazza, M., Mosher, D., Katz, M.E., Kent, D.V., Balini, M., 2014. A Middle–Late Triassic (Ladinian–Rhaetian) carbon and oxygen isotope record from the Tethyan Ocean. Palaeogeography, Palaeoclimatology, Palaeoecology 399, 246–259.

Pálfy, J., Zajzon, N., 2012. Envionmental changes across the Triassic-Jurassic boundary and coeval volcanism inferred from elemental geochemistry and mineralogy in the Kendlbachgraben section (Northern Calcareous Alps, Austria). Earth and Planetary Science Letters 335-336, 121–134.

Pálfy, J., Demény, A., Haas, J., Carter, E.S., Görög, A., Halász, D., Oravecz-Scheffer, A., Hetényi, M., Márton, E., Orchard, M.J., Ovárt, P., Vető, I., Zajzon, N., 2007. Triassic-Jurassic boundary events inferred from integrated stratigraphy of the Csővar section, Hungary. Palaeogeography, Palaeoclimatology, Palaeoecology 244, 11–33.

Piller, W., 1978. Involutinacea (Foraminifera) der Trias und des Lias. Beiträge zur Paläontologie von Österreich 1–164.

Reijmer, J.G., Everaars, J.S.L., 1991. Carbonate platform facies reflected in carbonate basin facies (Triassic, Northern Calcareous Alps, Austria). Facies 25, 253–278.

Reijmer, J.G., Betzler, C., Kroon, D., Tiedemann, R., Eberli, G.P., 1992. Bahamian carbonate platform development in response to sea-level changes and the closure of the Isthmus of Panama. International Journal of Earth Sciences (Geologische Rundschau) 91, 482–489.

Reijmer, J.G., Sprenger, A., Ten Kate, W.G.H.Z., Schlager, W., Krystyn, L., 1994. Periodicities in the composition of Late Triassic calciturbidites (Eastern Alps, Austria). Special Publications of the International Association of Sedimentologists 19, 323–343.

Richoz, S., Krystyn, L., 2015. The Upper Triassic events recorded in platform and basin of the Austrian Alps. The Triassic/Jurassic GSSP and Norian/Rhaetian GSSP candidate. Berichte der Geologischen Bundesanstalt 111, 75–136.

Richoz, S., Krystyn, L., von Hillebrandt, A., Martindale, R., 2012. End-Triassic crisis events recorded in platform and basin of the Austrian Alps. The Triassic/Jurassic and Norian/Rhaetian GSSPs. Journal of Alpine Geology 55, 321–374 (Field Trip Guide, 29th IAS Meeting of Sedimentology, Schladming/Austria).

Rigo, M., Bertellini, A., Concheri, G., Gattolin, G., Godfrey, L., Katz, M.E., Maron, M., Mietto, P., Muttoni, G., Sprovieri, M., Stellin, F., Zaffani, M., 2015. The Pignola-Abriola section (southern Appennines, Italy): a new candidate for the base of the Rhaetian stage. Lethaia 49, 287–306.

Ruhl, M., Kürschner, W.M., Krystyn, L., 2009. Triassic-Jurassic organic carbon isotope stratigraphy of key sections in the western Tethys realm (Austria). Earth and Planetary Science Letters 228, 169–187.

Satterley, A.K., 1996. The interpretation of cyclic successions of the Middle and Upper Triassic of the Northern and Southern Alps. Earth-Science Reviews 40, 181–207.

Satterley, A.K., Brandner, R., 1995. The genesis of Lofer cycles of the Dachstein Limstone, Northern Calcareous Alps. Geologische Rundschau 84, 287–292.

Sattler, U., Immenhauser, A., Hillgärtner, H., Esteban, M., 2005. Characterization, lateral variability and lateral extent of discontinuity surfaces on a carbonate platform (Barremian to Lower Aptian, Oman). Sedimentology 52, 339–361.

Schäfer, G., 1982. Geologische Karte der Republik Österreich, Blatt 96, Bad Ischl. Geologische Bundesanstalt, Wien.

Schlager, W., Reijmer, J.G., Droxler, A., 1994. Highstand shedding of carbonate platforms. Journal of Sedimentary Research B64 (3), 270–281.

Scholle, P.A., Arthur, M.A., 1980. Carbon isotope fluctuations in Cretaceous pelagic limestones; potential stratigraphic and petroleum exploration tool. American Association of Petroleum Geologists Bulletin 64 (1), 67–87.

Spötl, C., Vennemann, T.W., 2003. Continuous-flow isotope ratio mass spectrometric analysis of carbonate minerals. Rapid Communications in Mass Spectrometry 17, 1004–1006.

Swart, P.K., 2008. Global synchronous changes in the carbon isotopic composition of carbonate sediments unrelated to changes in the global carbon cycle. PNAS 105 (37), 13741–13745.

Tanner, L.H., 2010. The Triassic isotope record. In: Lucas, S.G. (Ed.), The Triassic Timescale. Geological Society, London, Special Publications 334, pp. 103–118.

Thibault, N., Ruhl, M., Ullmann, C.V., Korte, C., Kemp, D.B., Gröcke, D.R., Hesselbo, S.P., 2018. The Toarcian Oceanic Anoxic Event at Ravenscar (Yorkshire, UK) in its European context. Proceedings of the Geologists' Association 129, 372–391.

Van der Weijden, C.H., 2002. Pitfalls of normalization of marine geochemical data using a common divisor. Marine Geology 184, 167–187.

Weiland, T.E., 1991. Die Foraminiferen der Zlambachmergel des Rossmoosgrabens bei Bad Goisern, OÖ. (Obertrias, Nördliche Kalkalpen). Versuch einer paläoökologischen Interpretation. Diplomarbeit. Univ. Wien.

Weissert, H., 1989. C-Isotope stratigraphy, a monitor of paleoenvironmental change: a case study from the early cretaceous. Surveys in Geophysics 10, 1–61.

Whatley, R.C., 1988. Population structure of ostracods: some general principles for the recognition of palaeoenvironments. In: De Deckker, P., Colin, P., Peypouquet, J.P. (Eds.), Ostracoda in the Earth Sciences. Elsevier, Amsterdam, pp. 245–256.

Whiteside, J.H., Ward, P.D., 2011. Ammonoid diversity and disparity track episodes of chaotic carbon cycling during the early Mesozoic. Geology 39, 99–102.

Zaffani, M., Jadoul, F., Rigo, M., 2018. A new Rhaetian $\delta^{13}C_{org}$ record: carbon cycle disturbances, volcanism, End-Triassic mass Extinction (ETE). Earth-Science Reviews 178, 92–104.